
CHEMICAL COMPOSITION AND MICROSTRUCTURE OF RECENTLY OVIPOSITED EGGSHELLS OF *SALVATOR MERIANAE* (SQUAMATA: TEIIDAE)

FERNANDO H. CAMPOS-CASAL¹, FRANCISCO A. CORTEZ, ELIANA I. GOMEZ,
AND SILVIA N. CHAMUT

Cátedra de Biología del Desarrollo, Facultad de Agronomía y Zootecnia, Universidad Nacional de Tucumán,
Tucumán, Argentina

¹Corresponding author; e-mail: fhccasal@gmail.com

Abstract.—Reptiles are remarkable among amniotes, as they show reproductive heterogeneity ranging from egg-laying to live-bearing. In those species that are oviparous, the eggshell is an important physiological structure that connects the embryo with the physical environment of the nest. Knowing the structure and chemical composition of the eggshell is important for establishing specific and productive artificial incubation parameters that can help in the recovery of threatened or endangered natural populations. We examined the conformation and chemical composition of the eggshell of the Argentine Black and White Tegu (*Salvator merianae*) with optical microscopy, scanning electron microscopy (SEM), energy-dispersive X-ray spectroscopy (SEM-EDS), and Raman vibrational spectroscopy. The eggshell surface of *S. merianae* exhibits polygonal plaques separated by fissures. With the exception of a double layer of deep location compact fibers, the shell is mainly composed of alveolar fibrils. Histochemical analysis determined a dense layer of carbohydrates and/or sulfated mucins on the outer surface. The examination with SEM-EDS showed that the spatial distribution of Ca and P exhibits a strict coincidence in the superficial fissures and in the deep section of the shell. Using Raman vibrational spectroscopy, we determined that the only biomineral present in *S. merianae* eggshell is hydroxyapatite, whose location is consistent with SEM-EDS and light microscopy results. Together, these results provide a new perspective on the association between life-history strategies and eggshell types of reptiles.

Key Words.—biominerals; Black and White Tegu; hydroxyapatite; mucopolysaccharides; Raman spectroscopy; SEM-EDS

Resumen.—Los reptiles son notables entre las amniotas por su heterogeneidad reproductiva que va desde la puesta de huevos hasta nacimiento de crías vivas. En la modalidad ovípara, la cáscara del huevo es una importante estructura fisiológica que vincula al embrión con el ambiente físico del nido. Conocer la estructura y la composición química de la cáscara del huevo es importante para establecer parámetros de incubación artificial específicos que pueden ayudar con la recuperación de poblaciones naturales amenazadas. Examinamos la conformación y composición química de la cáscara de los huevos del lagarto overo argentino *Salvator merianae* con microscopía óptica, microscopía electrónica de barrido (MEB), espectroscopía de dispersión de rayos X (MEB-EDS) y espectroscopía vibracional Raman. La superficie de la cáscara de huevo de *S. merianae* exhibe placas poligonales separadas por fisuras. A excepción de una doble capa de fibras compactas de localización profunda, la cáscara está conformada principalmente por fibrillas alveolares. El análisis histoquímico determinó una capa densa de carbohidratos y/o mucinas sulfatadas en la superficie exterior. El examen con MEB-EDS mostró que la distribución espacial de Ca y P exhibe una estricta coincidencia en las fisuras superficiales y en la sección profunda de la cáscara. Utilizando espectroscopía vibracional Raman, determinamos que el único biomineral presente en la cáscara de huevo de *S. merianae* es hidroxiapatita, cuya localización es consistente con los resultados de SEM-EDS y de microscopía óptica. Estos hallazgos proporcionarían una nueva perspectiva sobre las estrategias reproductivas y los tipos de cáscara de huevo en los reptiles.

Palabras Clave.—biominerales; espectroscopía Raman; hidroxiapatita; lagarto overo; mucopolisacáridos; MEB-EDS

INTRODUCTION

Reptiles are a highly speciated group (Pyron et al. 2013), which occupy a fundamental position in the phylogeny of vertebrates and are notable for their dominant role and significant presence in many

environments (Reisz 1997). Most members of this class share basic reproductive and embryological attributes, evidence of their common ancestry (Stewart 1997; Blackburn 1998; Blackburn and Flemming 2009). Indeed, the most prominent plesiomorphic traits include sexual reproduction with internal fertilization and the

production of cleidoic eggs. The amniotic egg exhibits distinctive taxonomic characteristics such as a shell, synapomorphy typical of the Sauropsida (Mikhailov 1997; Norell and Xu 2005; Stein et al. 2019).

The amniotic eggshell is a microenvironmental compartment that physically protects the developing embryo, reduces the risk of serious damage during oviposition, and defends it against microbial invasion (Packard and DeMarco 1991; Benton 2005; Osborne and Thompson 2005; Hallmann and Griebeler 2015). It also modulates the exchange of water and gases between the egg and its environment (Packard et al. 1981; Booth and Yu 2008; Zhao et al. 2013; Tang et al. 2018) and provides an additional source of calcium during the embryogenesis. In most oviparous reptiles, the yolk supplies a significant amount of calcium to the embryo, whereas the calcium in the shell complements that of the yolk at the end of the incubation period (Packard and Clark 1996; Stewart et al. 2004; Sahoo et al. 2009; Jee et al. 2016). Particularly in the Squamata, the acquisition of embryonic calcium presents a variable pattern. Although it has only been studied in six snake species and 11 lizard species, the percentage of calcium provided by the yolk varies widely (Stewart and Ecay 2010; Stewart et al. 2019).

Morphologically, the eggshell in reptiles consists of an internal section (the surface adjacent to the albumin and to which the extra-embryonic membranes are attached) of heterogeneous conformation (Sexton et al. 1979; Trauth and Fagerberg 1984) named as inner boundary, boundary layer, or inner boundary layer (Packard et al. 1982a; Trauth and Fagerberg 1984; Schleich and Kästle 1988; Guillette et al. 1989; Hallmann and Griebeler 2015). The middle zone or interzone is made up of multiple layers of fibers that are interwoven, dispersed, or parallel to each other. The number of fibrous layers varies among species, and they also exhibit structural variation (Sexton et al. 1979; Yoshizaki et al. 2004; Kusuda et al. 2013; Chang and Chen 2016). Located on the outer surface, the inorganic eggshell layer is composed of calcium carbonate, such as calcite in crocodiles and Squamata, (Deeming 1988; Packard and Hirsch 1989; Packard and DeMarco 1991) or aragonite in Testudinidae eggs (Packard 1980; Silyn-Roberts and Sharp 1985, 1986; Al-Bahry et al. 2011).

Depending on the structure of the eggshell and the sensitivity of the egg to variations in the hydric environment (Kusuda et al. 2013), in Squamata it is possible to identify two types of conformation: the parchment-shelled eggs of snakes and most lizards (Packard and Packard 1980; Andrews and Sexton 1981; Packard et al. 1982b; Hirsch 1983) and rigid-shelled eggs found in Gekkonidae, Phyllodactylidae, and Sphaerodactylidae (Deeming 1988; Schleich and Kästle 1988; Pike et al. 2012; Hallmann and Griebeler 2015;

Choi et al. 2018). Parchment-shelled eggs consist of an inner boundary layer and a fibrous shell membrane, and rigid-shelled eggs are composed of a reticular bounding membrane, a dense fibrous interzone, and a calcareous shell layer. Although most representatives of the family Diplodactylidae lay soft eggshells, as an exception, some geckos of this same taxonomic category lay rigid eggshells that may have been independently acquired (Kratochvil and Frynta 2005).

Tegus (Squamata: Teiidae) of the genera *Salvator* and *Tupinambis* are the biggest lizards in South American and the most commercially exploited clade of neotropical reptiles (Murphy et al. 2016). The Red Tegu, *Salvator rufescens*, and the Black and White Tegu, *Salvator merianae* (Harvey et al. 2012), are the southernmost lizards in the genus and are distributed over a large fraction of Argentina, extending to northern Patagonia at about 40° south latitude (Manes 2016; Jarnevich et al. 2018).

Human activity has had a profound impact on the natural populations of tegus. In the past, native human communities used these lizards as a source of leather, meat, and fat (Norman 1987); however, this natural harnessing was dramatically altered by the disproportionate commercial exploitation of their skin (Chardonnet et al. 2002; Fitzgerald 2012). In South America from the 1970s to the 2000s, more than 34 million tegus skins were traded, about 1.02 million skins per year (Murphy et al. 2016). Particularly in Argentina, between the years 1975 and 1986, leather from more than 16 million tegus were exported legally, without illegal trafficking considered (Vieites et al. 2007). Currently, all members of the genus *Tupinambis* and *Salvator* are included in Appendix II of CITES (Convention on International Trade in Endangered Species of Wild Fauna and Flora; Manes 2016).

The sustainable breeding of *S. merianae* allows the economic and cultural use of this resource. Its rational exploitation under controlled conditions of captivity is also an economic alternative for native human communities, which in addition to raw and tanned skins, could add additional processing of meat and fat. The implementation of this breeding system requires knowledge and zootechnical management of diverse production parameters, such as artificial incubation. As we have explained above, the eggshell is an important functional barrier, which links the embryo to the environment. To know the conformation of this physiological structure would allow to consider the appropriate artificial incubation parameters for the embryonic development of *S. merianae*.

In oviparous species, the incubation regime during development influences short- and long-term phenotypic expression, including survival, hatchling size, post-hatch growth, locomotor performance, morphology and



FIGURE 1. (A) A female of Argentine Black and White Tegu (*Salvator merianae*) at the Experimental Lizard Hatchery of the Facultad de Agronomía y Zootecnia, Manantial 4105, Tucumán, Argentina. (B) A female *S. merianae* in its nesting and incubation chamber. (C) Eggs of *S. merianae*. Scale bar 2 cm. (Photographed by Eliana Gomez).

sex differentiation (Booth 2018; Ospina et al. 2018). This would suggest that incubation conditions can have potentially long-lasting effects in adult individuals. From a conservationist perspective, such phenotypic characteristics, optimized by artificial incubation, would be of fundamental consideration to repopulate and/or save threatened natural populations with captive-born individuals.

In our study, we analyzed the ultrastructure and histochemistry of recently oviposited eggshell of *S. merianae* using scanning electron microscopy (SEM)

and optical microscopy. Also, by using Scanning Electron Microscopy with Energy Dispersive Spectroscopy (SEM-EDS), we evaluated the spatial distribution and relative composition of Mg, P, Ca, and S; elements particularly important for skeletogenesis and eggshell structuring. Finally, we identified the chemical nature of the calcium material with Raman vibrational spectroscopy.

MATERIALS AND METHODS

Animals, handling, and housing.—We obtained 24 eggs from six nests built by *S. merianae* females (with at least two previous layings). The average weight of females was 4 kg and average snout-vent length was > 35 cm (Fig. 1A). After mating, we housed the females in individual nesting enclosures with an incubation chamber (Fig. 1B). We housed the animals at the Experimental Lizard Hatchery of the Facultad de Agronomía y Zootecnia of the Universidad Nacional de Tucumán, located at Finca "El Manantial" (26°51'S, 65°17'W), province of Tucumán, Argentina.

Eggshells.—The shape of the *S. merianae* eggs were an ellipse with an average length of 40 mm and the average radius of 12.5 mm (Fig. 1C). The shell of recently oviposited eggs were whitish (Fig. 1C), soft and very flexible, and with a thickness of 180 μ m. To exclude possible modifications in the morphology and chemical composition of the shell associated with embryonic development or incubation, we used recently oviposited eggs (up to 12 h after laying) in a perfect preservation status.

Optical microscopy.—For histochemical studies, we immersed 12 whole eggs in 4% formaldehyde solution in phosphate-buffered saline at pH 6.8 (Suvarna et al. 2008) for 24 h at 4° C. After that, we cut with fine-tipped scissors the shell perpendicularly to the plane of the minor axis, divided the shell into two halves, and preserved the shell in 70% ethanol. We did not include the portion of eggshell in contact with the embryo. We dehydrated small pieces of shell of each egg ($n = 24$) in alcohol, diaphanized them in xylene, included them in paraffin-celoidin and serially sectioned them at 8 μ m.

We determined acid mucins and mucopolysaccharides with Alcian Blue 8GX (AB; Sigma-Aldrich, Buenos Aires, Argentina). We stained the sections for 15 min in a solution of 1% AB, pH 1.0 and pH 2.5 (Suvarna et al. 2008), drained and air dried the sections, rapidly dehydrated them in absolute ethyl alcohol, and cleared and mounted sections. To identify the type of the acid groups in the mucopolysaccharides (carboxyl or sulphate), we treated the eggshell sections with an acidified methanolic solution (Martoja and Martoja

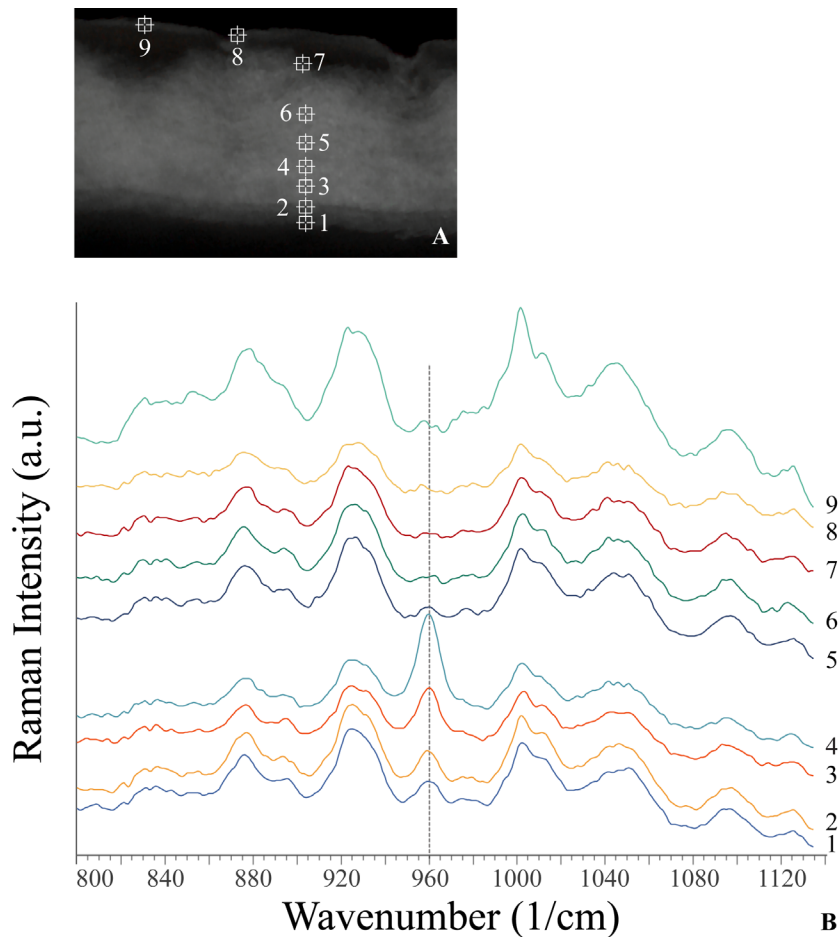


FIGURE 2. Spectral sampling in a radial slice of the eggshell of the Argentine Black and White Tegu (*Salvator merianae*). (A) Microphotography of a radial section of the eggshell indicating the nine sampling points corresponding to spectra 1–9 in image B. Outside of eggshell is up. (B) Spectral region between 800 and 1140 cm^{-1} . Notice the behavior of the band at 960 cm^{-1} according to the position of the sampled point.

1970). After that we stain the methylated samples in a solution of 1% AB, pH 1.0 or pH 2.5 (Suvarna et al. 2008).

We performed a histochemical determination of calcium with 1% Alizarin Red S (AR; Biotech, Buenos Aires, Argentina) with a pH of 4.3 for 4–5 min (Martoja and Martoja 1970). We used as controls decalcified sections of shell using 5% nitric acid for 30 min at 60° C, stained the sections with AR, and contrasted the shell sections with eosin and AB (pH 2.5). Afterwards, we rapidly dehydrated the sections in acetone, and cleared and mounted them. We photographed sections with an Olympus BX51 microscope (Olympus Corporation, Tokyo, Japan) equipped with an Olympus Q Color 5 digital camera controlled with Pro Express 6.0 software (Media Cybernetics, Rockville, Illinois, USA).

SEM and SEM-EDS.—We fixed 12 small eggshell sections in half-concentration Karnovsky's fixative (Karnovsky 1965) for 24 h at 4–5° C. Afterwards, we dehydrated the pieces in ethanol and acetone, and

dried them by critical point. Then we coated them with gold and observed sections with a Zeiss Supra 55VP scanning electron microscope (Carl Zeiss, Oberkochen, Germany) with Smart SEM 5.05 operating software (Carl Zeiss).

We determined the percentage weight and spatial distribution of Ca, P, Mg, and S by Energy-Dispersive X-ray Spectroscopy (EDS) using an EDS detector (INCA PentaFET-x3, Oxford Instruments, Abingdon, UK) with INCA Suite 4.13 software (Oxford Instruments) coupled to a SEM Zeiss Supra 55VP. The setting of EDS analysis was an accelerating voltage 10.0 kV and a working distance 8.5 mm. We calibrated the EDS prior to each analysis using pure cobalt and we mapped areas of interest for 2 min.

Raman vibrational spectroscopy.—We carried out spectroscopic examination at different points of the eggshell, both in radial sections ($n = 24$) and on the outer surface, with a DXR Smart Raman instrument (Thermo Fisher Scientific, Waltham, Massachusetts,

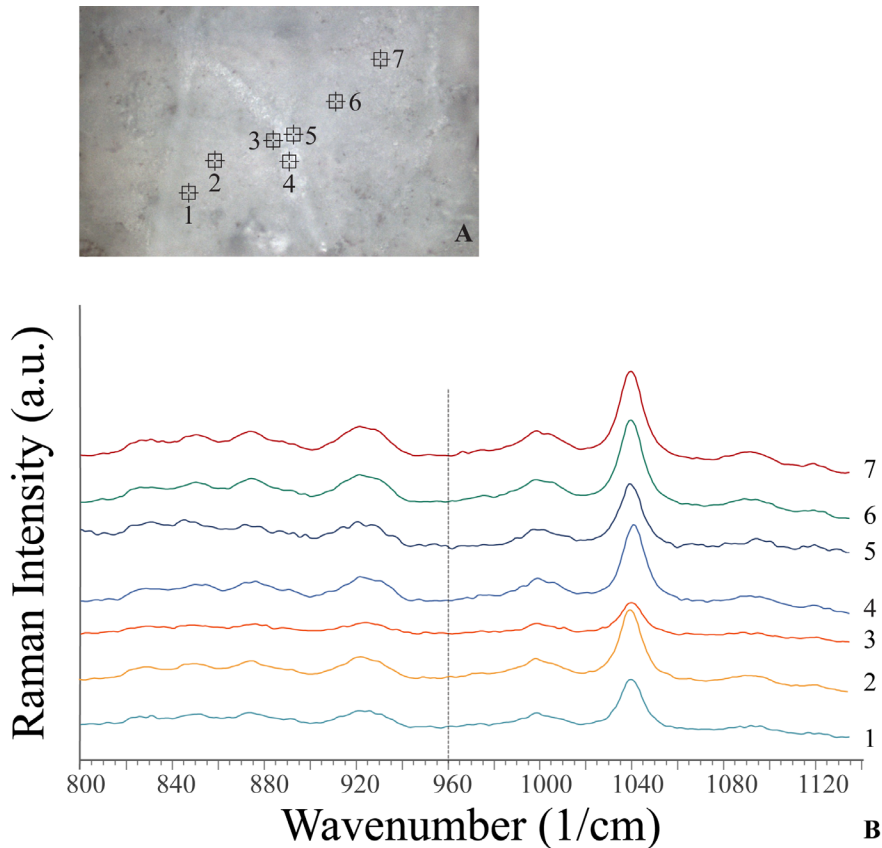


FIGURE 3. Spectral sampling of the outer surface of the eggshell of the Argentine Black and White Tegu (*Salvator merianae*). (A) Microphotography of the outer surface of the eggshell indicating the seven sampling points corresponding to spectra 1 to 7 in image B. (B) Spectral region between 800 and 1140 cm^{-1} . Notice the absence of the spectral band at 960 cm^{-1} at all sampled points.

USA) equipped with a 780 nm excitation wavelength at 24 mW of power (4 cm^{-1} spectral resolution). We used a confocal aperture of 50 μm slit for data collection. We focused samples with a $20\times$ objective. Each sampling point yielded one individual-spectrum, which we acquired by accumulating 100 expositions with an exposure time of 5 s each.

The control tests consisted of the vibrational analysis of the mineralized fraction of six eggshell pieces of domestic Chickens (*Gallus gallus*) and of the enamel of tooth pieces of *S. merianae*. For this purpose, we used six robust unicuspid teeth (Brizuela and Albino 2010) from three specimens of both sexes and different ages of *S. merianae*, which we euthanized in the framework of other studies. We anesthetized the animals with diazepam (2.5 mg/kg) and intramuscular ketamine (25 mg/kg) and euthanized them with intracardiac injections of sodium pentobarbital (100 mg/kg; Baer 2006). We extracted teeth with forceps and sectioned them with an electric lathe equipped with a circular toothed mini saw. We processed all spectral data with the OMNIC 8.3 software suite (Thermo Fisher Scientific).

The determination of the chemical nature of the calcium material was performed by spectral sampling of

the radial sections (Fig. 2A) and the outer surface (Fig. 3A) of *S. merianae* eggshells. We sampled eggshell radial sections ($n = 24$) at nine points. We selected the points sampled (Fig. 2A) considering the fibrillar distribution and the location of the calcium deposit in the eggshell. From inner to outer surface, sampling points one and two were located in the double layer of fibers in the deep zone of the shell. Points three, four, and five correspond to the region of the calcium deposit in the deep section of the interzone. In particular, we located the sampling point five at the transition between the calcium deposit and the adjacent fibrillary region. We sampled points six and seven in the surface interzone. Finally, we located sampling points eight and nine at the base of a fissure and on an adjacent polygonal plaque (Fig. 2A).

On the outer surface of the eggshell ($n = 12$), we performed the spectral analysis at seven points. From left to right (Fig. 3A), points one, two, six, and seven correspond to the samples performed in two contiguous polygonal plaques. Points three and five correspond to the transition zones between the edges of the plaque and the fissure. Finally, point four was sampled in the center of the fissure (Fig. 3A). To improve results in

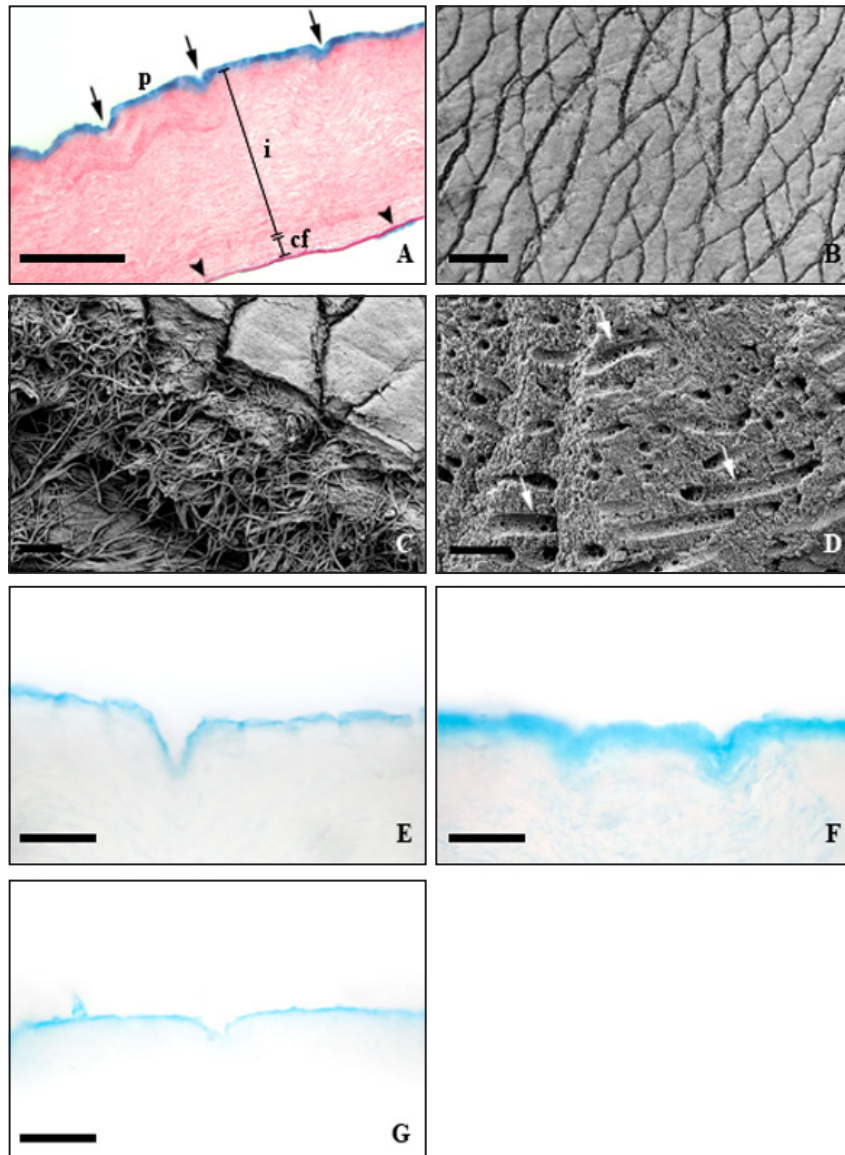


FIGURE 4. Scanning electron and light microscopy micrographs of Argentine Black and White Tegu (*Salvator merianae*) eggshells. (A) Light microscope microphotography cross section of eggshell co-stained with eosin and AB pH 2.5. The arrows point to the fissures. Note the plaques (p) between the fissures. The arrowheads indicate the inner boundary layer. i, interzone; cf, compact fibres. Scale bar 90 μm . (B) Outer surface of shell. Scale bar 300 μm . (C) Fibrillary network connected to the outside through fissures. Scale bar 60 μm . (D) Detail of the granular interstitial cement. Notice the imprint of the fibers on the inter-fibrillar material (arrows). Scale bar 3 μm . (E) Light micrograph of a cross-section through eggshell stained with AB pH 1. Scale bar 30 μm . (F) Light micrograph of a cross-section through eggshell stained with AB pH 2.5. Scale bar 30 μm . (G) Light micrograph of a cross-section through eggshell, methylated, and stained with AB pH 2.5. Scale bar 30 μm . In all images, the outside of eggshell is up. (E, F, and G photographed by Fernando Campos-Casal).

comparing, adding, and subtracting spectra, we use the OMNIC 8.3 software baseline correction tool. We carried out all spectroscopic experiments at ambient temperature.

Terminology.—In this paper, we adopt only some terms used in the description of reptilian eggshells (Sexton et al. 1979; Schleich and Kästle 1988; Packard and DeMarco 1991). We only used the inner boundary layer designation to indicate the inner section of the

shell in contact with the vitelline membrane of the egg. We use the name interzone to refer to the fibrillary section of the egg between the outer surface and the inner boundary layer.

RESULTS

SEM and histochemistry morphological observations.—The outer surface of the oviposited egg of *S. merianae* exhibits irregularly shaped polygonal

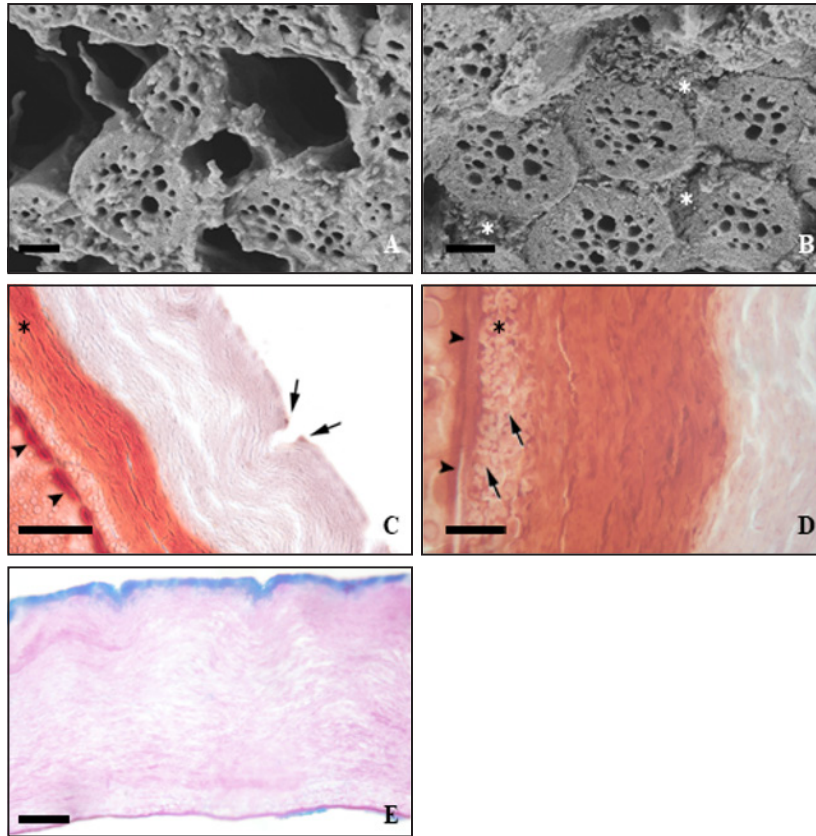


FIGURE 5. Scanning electron microscopy of the alveolar fibers of the interzone and light microscopy micrographs of Argentine Black and White Tegu (*Salvator merianae*) eggshells. (A) Groups of alveolar fibers from the outer surface area of the eggshell separated by large inter-fibrillar spaces. Scale bar 0.6 μm . (B) Alveolar fibers from the deep eggshell area surrounded by occlusive interfibrillar material. The asterisks indicate the calcium interfibrillar material. Scale bar 0.6 μm . (C) Light micrograph of a cross-section through eggshell stained with AR. Notice the calcium band in the deep zone of the shell (asterisk). The edges of the outer surface furrows are slightly reactive (arrows). The arrowheads point to the inner boundary layer. Scale bar 56 μm . (D) Note the calcium deposit (arrows) between the compact fibers in the deep zone of the eggshell (asterisk), adjacent to the inner boundary layer (arrowheads). Scale bar 15 μm . (E) Light micrograph of a cross-section through eggshell decalcified, co-stained with eosin and AB pH 2.5. Scale bar 40 μm . (Figures C, D, and E photographed by Fernando Campos-Casal).

sections divided by fissures or channels (Fig. 4B). This discontinuous coating covers a dense network of 0.16 μm diameter fibrils (Fig. 4C), embedded in amorphous material of granular appearance (Fig. 4D). The fissures or channels connect the free surface of the eggshell to the underlying inter-fibrillary network (Fig. 4C).

We characterized the glyconjugates of the shell by selective staining with AB at pH 1 and 2.5. In the sections incubated with AB pH 1 we found the presence of sulfomucins and/or sulfated proteoglycans revealed as a thin layer of 4 μm thickness and restricted to the outer surface region of the eggshell (Fig. 4E). Using AB in pH 2.5, we found a consistent cortical zone of 11 μm thickness (Fig. 4F) formed by sulfomucins and/or sialomucins. Inside, the fissures are also positive for staining with AB at both pH 1 and pH 2.5. The loss of AB reactivity at pH 2.5 by methylation suggests the presence of carboxylated carbohydrates and/or sulphated mucins in the surface layer of the eggshell (Fig. 4G).

Most of the eggshell thickness (85%) consisted of a wavy mesh of parallel fibers (Fig. 4A) that were unbranched and included in an amorphous matrix. The ultrastructure of these fibrils with diameters between 1.4–2.0 μm was characterized by the existence of numerous intrafibrillary alveoli (Fig. 5A, B). The transition to the middle zone of the eggshell was determined by the compaction of the interstitial material. In fact, in the outermost region of the eggshell, the amorphous material exhibited numerous cavities that separated small groups of fibers (Fig. 5A). Progressively, towards the deepest region, the inter-fibrillary interstices were reduced, and the amorphous calcium component was evidenced as an occlusive peripheral material (Fig. 5B).

We found the presence of a conspicuous deposit of calcium material of 43–55 μm thickness using AR, occurring in the deepest region of the interzone of the eggshell (Fig. 5C, D). In addition, the absence of staining in the decalcified sections supports this result

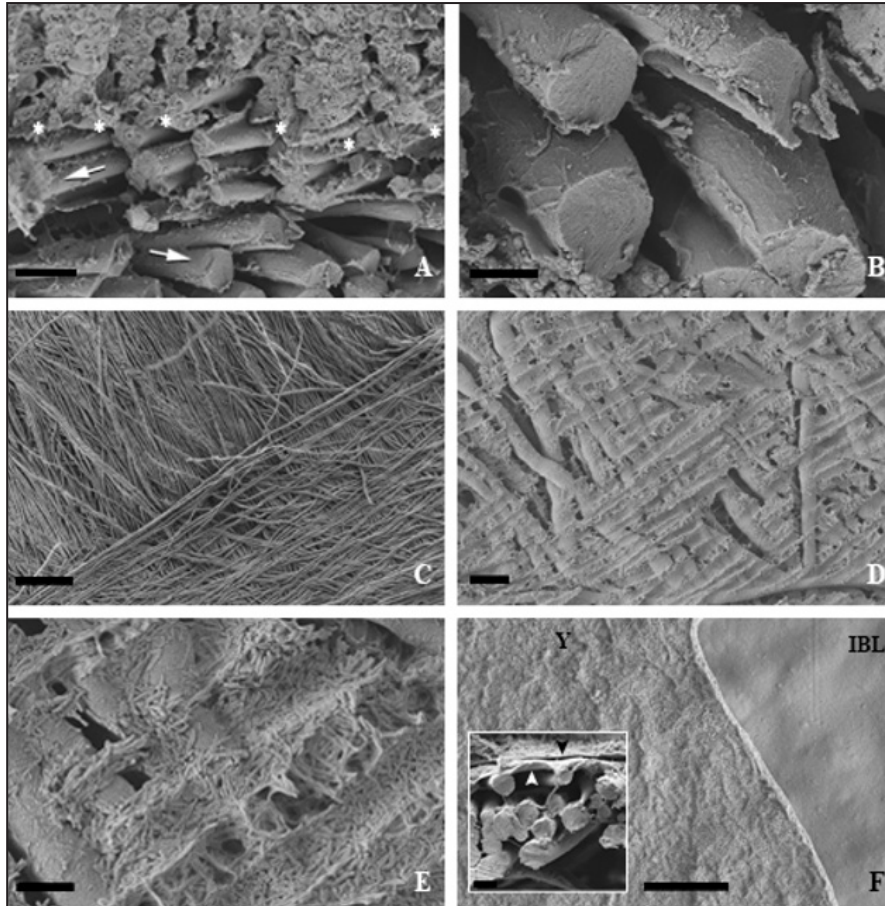


FIGURE 6. Scanning electron micrographs of the deep shell region of the egg of Argentine Black and White Tegu (*Salvator merianae*). (A) Radial section showing alveolar fibers in deep interzone and compact fibers arranged in a double layer. Note the orthogonal arrangement of the fibers (arrows). The asterisks indicate the boundary between the deep interzone and compact fibers. Outside of eggshell is up. Scale bar 4 μm , (B) Detail of the compact fibers. Scale bar 1.6 μm , (C) Top view of the inner layer organized as a double fibrillary layer. Scale bar 50 μm , (D) Top view of the inner layer delaminated. Notice the impressions of the fibers on the interfibrillary material. Scale bar 5 μm , (E) Detail of the image D. Notice the morphology of the interfibrillary material. Scale bar 1.5 μm , (F) Partial removal of the vitelline membrane with residual yolk (Y) exposes the inner boundary layer (IBL). Scale bar 6 μm . In the insert the vitelline membrane (black arrowhead) is observed in contact with the inner boundary layer (white arrowhead) attached to the compact fibers. Scale bar 2 μm .

(Fig. 5E). We also found the presence of small nuclei sensitive to alizarin at the edges of the furrows of the superficial stratum of the eggshell (Fig. 5C).

In the deepest region of the eggshell, the ultrastructural examination revealed the presence of an inner layer (10% of thickness) made up of two sheets of compact fibers (Fig. 6A) of 2.6 μm diameter (Fig. 6B), with an orthogonal arrangement between them (Fig. 6A, C). When both sheets are manually dissociated, we observed wide inter-fibrillary spaces (Fig. 6D) occupied by interstitial material with the appearance of rods (Fig. 6E). In contrast, the analysis of the sections stained with AR showed the presence of calcium material deposited in the inter-fibrillar matrix in the compact fiber layer (Fig. 5D). The inner boundary layer of the shell was a thin continuous membrane of homogeneous appearance (Fig. 6F). While one side of this sheet was anchored to the compact fibers, the opposite side was closely linked

to the vitelline membrane of the oocyte (Fig. 6F, insert). Our ultrastructural examination with SEM did not reveal the presence of fibers in this area.

SEM-EDS.—Notably on the outer surface of the eggshell (Fig. 7A), the qualitative analysis showed that Ca and P exhibited a similar spatial distribution pattern, located at the fissures (Fig. 7C, D). The quantitative results revealed 2.2 and 1.32 percentage weight of Ca and P, respectively (Table 1). Although S exhibited a quantitatively high proportion (percentage weight 3.42; Table 1) its spatial distribution on the eggshell surface did not show any discernable pattern (Fig. 7B). At least in the detection range of SEM-EDS, we did not detect a Mg signal on the outer surface of the shell of *S. merianae* egg (Table 1).

Mapping the radial sections of the eggshell (Fig. 8A) showed that Ca and P exhibited a repetitive spatial

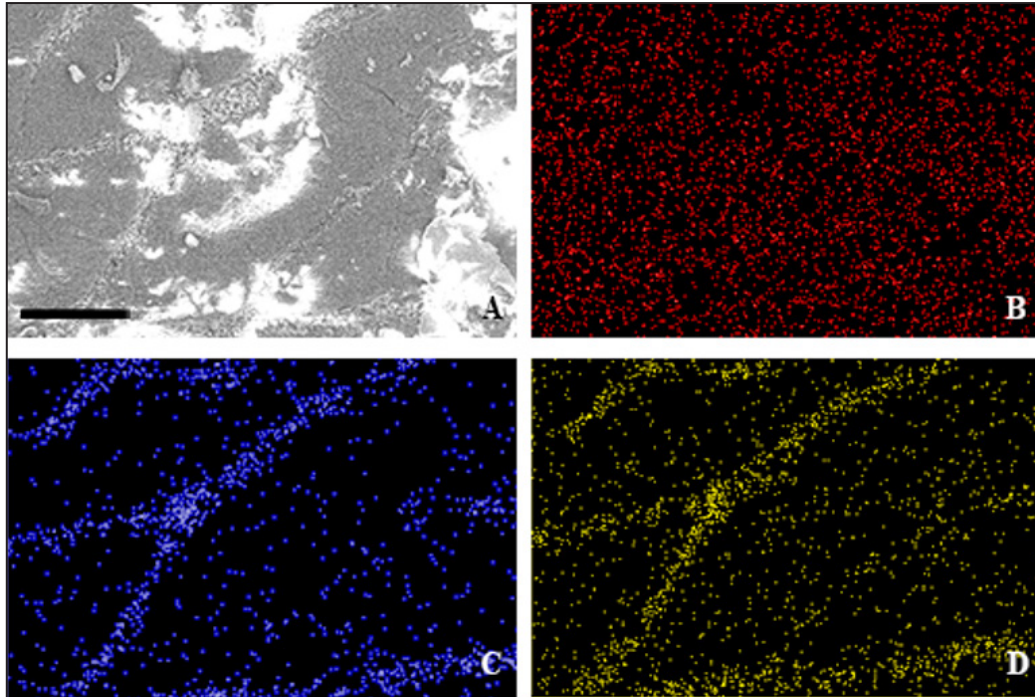


FIGURE 7. Elemental mapping images of the eggshell outer surface of the Argentine Black and White Tegu (*Salvator merianae*). (A) Surface view of the eggshell. (B, C and D) Spatial distribution of S, Ca and P, respectively. The S exhibits a uniform monotonous distribution pattern. Notice the overlapping of P and Ca in the fissures. All images are on the same scale (scale bar 100 μm).

distribution pattern on the surface and in the middle section of the interzone (Fig. 8C, D); however, in the deep zone, the distribution maps of both elements were substantially amplified, coinciding as an intense band of 44–57 μm thickness, in morphological correspondence with the deep interzone and the double layer of compact fibers (Fig. 8C, D). The quantitative results also revealed 2.94 and 2.43 percentage weight of Ca and P, respectively (Table 1). In addition, the mapping revealed Ca and P signals, morphologically associated to surface fissures (Fig. 8C, D). The location and extent of calcium material at deep interzone, as well as the presence of calcium at the fissures, are consistent with the results obtained using AR (Fig. 5C). Although S and Mg are present throughout the eggshell thickness, they lack a specific distribution pattern (Fig. 8B, E). Quantitative analysis indicated a high proportion of S and traces of Mg (Table 1).

Raman vibrational spectroscopy.—The spectra of the calcium deposit (Fig. 2A, sampling points 1–5; Fig. 2B, spectra 1–5) revealed a characteristic band located at 960 cm^{-1} . A larger proportion of this band in spectrum four was noticeable, in contrast with spectra one, two, three and five, respectively. Conversely, in the spectra of the regions corresponding to the most superficial and outer interzone (Fig. 2A, sampling points 6–9; Fig. 2B, spectra 6–9), the spectral band at 960 cm^{-1} was virtually absent.

To confirm that the observed band corresponds to hydroxyapatite, we made a subtraction between spectrum four, characterized by the conspicuous signal at 960 cm^{-1} , and spectrum six; corresponding to the first point of the series of samples that lacks this band (Fig. 9; #4-6). With this subtraction procedure, we eliminated the bands corresponding to the organic components and exposed more clearly the vibrational peak at 960 cm^{-1} . We compared the derived spectrum with the hydroxyapatite control spectra of the tooth enamel of *S. merianae* and calcite of the eggshell of *Gallus gallus* (Fig. 9). The spectral band of the hydroxyapatite of the teeth was similar to the vibration pattern observed in the eggshell at 960 cm^{-1} , corresponding to the symmetrical stretch PO_4^{3-} (Fig. 9; Nosenko et al. 2016). In addition, it was possible to identify in the spectrum #4-6 two

TABLE 1. Quantitative proportion of S, Ca, P, Mg on the outer and inner surface of the shell of the Argentine Black and White Tegu (*Salvator merianae*) eggs.

| Element | Outer Surface | | Inner Surface | |
|---------|---------------|----------|---------------|----------|
| | Weight % | Atomic % | Weight % | Atomic % |
| S | 3.42 | 1.73 | 2.43 | 1.06 |
| Ca | 2.2 | 0.89 | 2.94 | 1.03 |
| P | 1.32 | 0.69 | 2.43 | 0.8 |
| Mg | 0.00 | 0.00 | 0.08 | 0.04 |

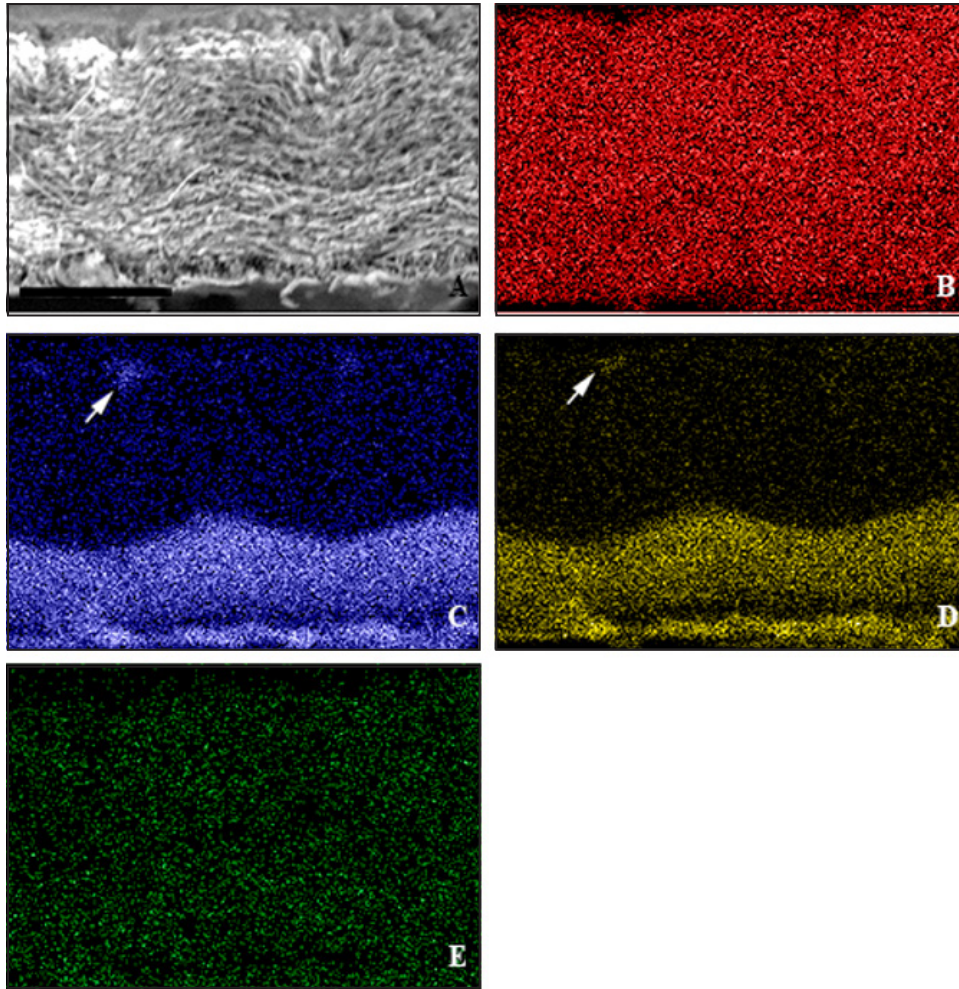


FIGURE 8. Elemental mapping images of the shell of the recently oviposited egg of Argentine Black and White Tegu (*Salvator merianae*). (A) Radial section of shell. (B, C, D, and E) Spatial distribution of S, Ca, P, and Mg, respectively. Note the similar pattern of spatial distribution of Ca and P in the inner region of the shell, as well as at the edges of the fissures (arrows). S and Mg exhibit a monotonous distribution pattern. All images are on the same scale (scale bar 100 μm). Outside of eggshell is up.

additional weak bands at 429 and 587 cm^{-1} , due to the deformations of the PO_4^{3-} groups (Fig. 9; Timchenko et al. 2018). The band at 1,069 cm^{-1} of the tooth enamel agree with the stretching of the CO_3^{2-} groups, characteristic of carbonated hydroxyapatite (Fig. 9; Timchenko et al. 2018).

The contrast between the #4-6 spectra and the calcium carbonate control spectrum of the *Gallus gallus* eggshell showed that none of the acute and intense bands at 1,085, 710, 280 and 152 cm^{-1} , characteristics of the calcite (De La Pierre et al. 2014), are present in the eggshell of *S. merianae* (Fig. 9). On the outer surface of the eggshell, none of the spectra (Fig. 3B) of the seven sampling points (Fig. 3A) showed a characteristic hydroxyapatite or calcite vibrational pattern (Fig. 9). To confirm the existence of weak signals of these biominerals, we intensified the vibrational signal by the sum of the seven spectra of the outer surface of the shell (Fig. 3B). The

sum spectrum (#1+7; Fig. 9) did not show vibrational peaks of hydroxyapatite and/or calcite.

DISCUSSION

The structure and composition of the eggshell of reptiles is heterogeneous and encompasses a wide range of types, from flexible parchment-shelled eggs to rigid-shelled eggs. Although these categories are generalizations based on morphological similarities, they have provided an excellent frame of reference to explain the response of eggs and embryos to variations in the nest hydric microenvironment during incubation (Packard et al. 1982b, 1991). We found that the free surface conformation of the *S. merianae* eggshell is similar to that observed in the Zebra-Tailed Lizard (*Callisaurus draconoides*; Packard et al. 1982a), the Slender Anole (*Anolis limifrons*) and the Bahaman

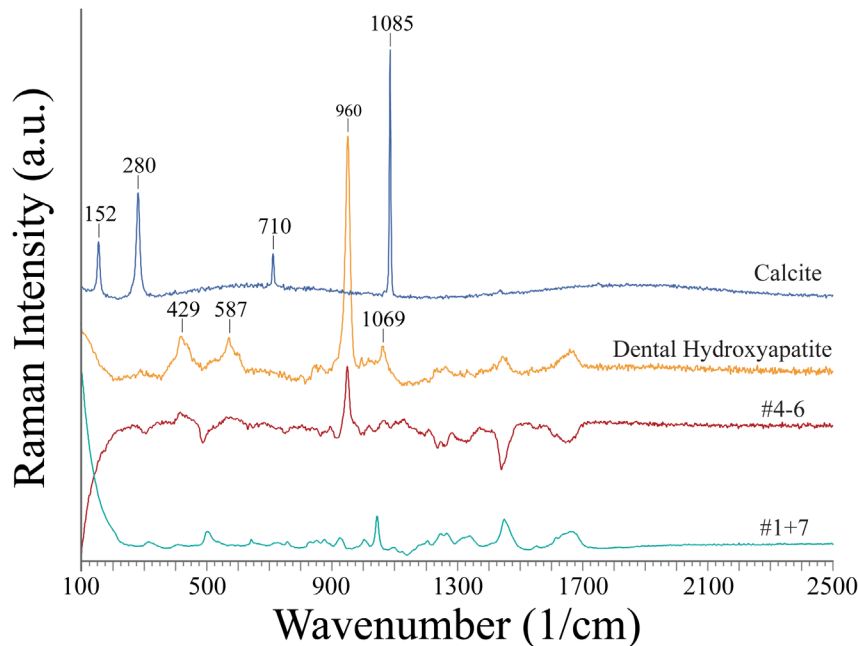


FIGURE 9. Comparison between the sum spectrum of the shell surface (Fig. 3B; #1+7), the spectrum difference between the spectra 4 and 6 (Fig. 2B; #4–6) of the interzone with the spectra corresponding to the hydroxyapatite controls of the Argentine Black and White Tegu (*Salvator merianae*) dental enamel and calcite of the Chicken (*Gallus gallus*). Note the absence of the typical vibrational peaks of calcite (152, 280, 710 and 1,085 cm^{-1}) on the inner and outer surface of the eggshell of *S. merianae*.

Brown Anole (*Anolis sagrei*; Sexton et al. 1979; Schleich and Kästle 1988), the Desert Iguana (*Dipsosaurus dorsalis*; Packard et al. 1982b), and the Eastern Six-Lined Racerunner (*Aspidozelis sexlineatus*; Trauth and Fagerberg 1984). Inside, the eggshell of *S. merianae* is composed of several layers of alveolar fibers and a double layer of compact fibers, both immersed in an amorphous inter-fibrillary matrix. Alveolar fibers have been observed also in the eggshells of other Squamates (Sexton et al. 1979; Packard et al. 1982a; Trauth and Fagerberg 1984; Heulin 1990; Trauth et al. 1994).

From the functional viewpoint, it has been suggested that intrafibrillary cavities provide a potential space for water storage, helping with the water balance of the egg (Trauth and Fagerberg 1984). In fact, approximately 85% of the thickness of the eggshell of the *S. merianae* is made up of alveolar fibers, a significant proportion that could be associated with this function, considering the high humidity of the nests of these lizards (Manes 2016). It has also been proposed that these alveolar fibrils would provide thermal insulation against abrupt temperature changes during incubation (Trauth and Fagerberg 1984; Trauth et al. 1994). A notable discovery has revealed that *S. merianae* can generate heat using endothermia during its reproductive period (Tattersall et al. 2016). Compared to other lizards, this finding is unique. *Salvator merianae* is able to modify its body temperature, cyclically during the day, up to 10° C above the environmental temperature (Tattersall et al. 2016). In addition, in this same lizard, it has been demonstrated

that nests naturally incubated by females have an average temperature 5° C higher than empty nests (Manes et al. 2003). Although there are no unequivocal results concerning the thermal resistance of alveolar fibers, it would be reasonable to consider that these fibers would protect the embryo from being diverted from its optimal developmental temperature caused by maternal thermal variations. Temperature-induced anomalies have been observed in reptile embryos as a result of both sub- and supra-optimal temperatures (Vinegar 1974; Muth 1980). Malformations related to the abdominal wall, head, skull, and limb malformations were also identified in poultry eggs induced by thermal stress (Noiva et al. 2014).

The presence of compact fibers, arranged as a simple layer, contiguous with the inner boundary layer, have been referred to in other iguanids (Sexton et al. 1979; Trauth and Fagerberg 1984; Schleich and Kästle 1988; Trauth et al. 1994). In this work we have determined in the eggshell of *S. merianae* a double layer of compact fibers with orthogonal arrangement. In general, it has been established that Squamata eggshell fibers, besides providing structural support, allow the egg to adjust to volumetric changes during incubation (Sexton et al. 1979). Several researchers have focused on this function; however, they have not provided conclusive data on the structural and mechanical properties of the fibers. Chang and Chen (2016) have shown that the eggshell of the Chinese Cobra (*Naja atra*) is composed of keratin fibers and a smaller proportion of collagen

fibers, which together give the shell an exceptional deformability. The double layer of compact fibers that we have documented in *S. merianae* exhibit a location and spatial organization similar to that observed in *Naja atra*. The layers consist of plywood structured collagen fibers, capable of supporting a great traction force (Chang and Chen 2016). In a detailed work concerning to the formation and structure of eggshells in oviparous reptiles, Packard and DeMarco (1991) pointed out that the eggs of all Squamata have a superficial layer (calcareous layer) composed of calcium carbonate. The results presented here differ from this generalization.

Through Raman vibrational spectroscopy, we demonstrated a strict coincidence between the spectrums of the areas with high concurrence of Ca and P in the eggshell and the spectrum of the dental hydroxyapatite of *S. merianae*. In addition, the absence of vibrational peaks, characteristic of calcite (De La Pierre et al. 2014), both on the outer surface and inside of the eggshell, allow us to rule out the existence of this salt in the eggshell of *S. merianae*. Furthermore, the spectra are lacking in vibrational peaks at 950 cm^{-1} , characteristic of the P-O stretching of amorphous calcium phosphate (Saber-Samandari et al. 2014; Stammeier et al. 2018). The absence of hydroxyapatite vibrational peaks in the fissures and plaques would be linked to the low signal of Ca and P observed in the SEM-EDS mapping.

The glycosaminoglycans of the *S. merianae* eggshell constitute an uninterrupted dense cover between the plaques of the outer surface and the open fissures to the underlying fibrillary network. The presence of carboxylated glycosaminoglycans and/or sulfomucins in the eggshell outer surface of reptiles has not been previously reported. In comparison, the outermost layer of the egg shell in birds known as cuticle layer, cuticle, cover or segment (Arias et al. 1993) is composed mainly of mucin in the form of high molecular weight glycoconjugates with numerous disulfide bonds, free sulfhydryl groups (Roussel et al. 1988), and sialic acid (Wedral et al. 1974). Hyaluronan, chondroitin sulfate, heparan sulfate, and keratan sulfate have been characterized in both the membranous and calcareous fraction of chicken eggshells (Liu et al. 2014). Indeed, the high degree of glycosidation of the cuticular cover has been shown to be an important characteristic of the eggshell of birds to resist bacterial attack (Rodríguez-Navarro et al. 2013). Presumably, in the absence of a calcareous layer on the shell of the oviposited *S. merianae* egg, the gelling property of glycosaminoglycans would establish a defensive barrier against attack by microorganisms and cooperate with the appropriate water balance required in the parchment-shelled eggs.

The eggshell as a source of Ca and P required for skeletogenesis has been studied in reptiles (Stewart and Ecay 2010; Jee et al. 2016). Vibrational spectra of *S.*

merianae eggshells show that Ca and P are chemically associated as hydroxyapatite, whose location is consistent with the spatial distribution determined with AR, a very reliable stain for visualizing calcium salts even in small amounts (Suvarna et al. 2008). We also demonstrated the absence of typical spectral signals of hydroxyapatite or amorphous calcium phosphate in the intermediate and upper sections of the interzone of the eggshell of *S. merianae*. In addition, SEM-EDS mapping showed that, in these same areas, Ca and P exhibit a regular distribution pattern. Together, these results allow us to tentatively conclude that at least a fraction of Ca and P from the eggshell of *S. merianae* would be present as chemical elements.

Quantitative SEM-EDS analysis also showed traces of magnesium (0.08 percentage weight) in the inner surface of eggshell of *S. merianae*. At present, we do not know the factor(s) that would determine such a low Mg content in the shell of *S. merianae*. Studies on the role of Mg in bone biomineralization showed that high concentrations of this element inhibit the crystallization of hydroxyapatite in vivo (Zhang et al. 2019), by partially replacing Ca^{2+} ions in the apatite structure (Combes and Rey 2010). In this context, it could be considered that the limited amount of Mg in the recently deposited eggshell of *S. merianae* would be appropriate to promote a normal biomineralization of hydroxyapatite.

Among the elements analyzed, S could be considered as representative of the organic content of the eggshell. Thus, the high level of S determined by SEM-EDS (2.43 percentage weight) in the *S. merianae* eggshell would be linked to the protein fibrillar structure. Likewise, S is usually linked with keratin-associated proteins characteristic for its important cysteine content (Rogers et al. 2006), an amino acid that has been determined in a wide variety of eggshells in Squamates (Sexton et al. 2005). Choi et al. (2018) have shown that the maximum concentration of S (2.0–2.5 percentage weight) in the egg of gekkotids is located in the non-calcified section of the shell in soft-shelled eggs. Possibly, the high S content in the surface layer (3.42 percentage weight) of the *S. merianae* eggshell is involved in the formation of the sulfated polysaccharide coating that we have determined.

Taken together, the studies presented here raise questions about the biology of the *S. merianae* egg. As we have noted, Ca and P exist in the eggshell combined as hydroxyapatite and possibly as free chemical elements. This duality raises the question about the bioavailability of these sources during embryogenesis. In accordance with the eggshell morphology and maternal influence, under controlled incubation conditions, two reciprocal interaction factors should be considered: water and temperature. Indeed, temperature has an intense impact

on the water balance of the egg, mainly altering the rate of diffusion of water vapor through the eggshell (Packard 1991). On the other hand, the modification or stabilization of nest temperature substantially accelerates or alters the development rates of embryos in reptiles (Farmer 2003). Furthermore, alterations of sex ratios induced by temperature of incubation (Booth 2018) would be important for the zootechnical management of *S. merianae*.

Artificial incubation is a fundamental aspect of any breeding program with conservation objectives. The artificial incubation of *S. merianae* eggs and the management of animals hatched in captivity would allow the sustainable use of this species and would have a more visible impact on its conservation than simply restricting hunting (Manes 2016). Advances in this field of zootechnical application could be extended to the conservation of *S. rufescens*, another species of tegu widely distributed in Argentina.

Acknowledgments.—This paper has been partially funded by PIUNT Project 26/A605 to the Secretaría de Ciencia, Arte e Innovación Tecnológica (SCAIT) of the Universidad Nacional de Tucumán. We are especially grateful to Dr. María Rosa Álvarez and Licenciada Doly Chemes of Laboratorio de Espectroscopia Raman, (LERA-CONICET) for their dedication and for their technical assistance during Raman measurements. We thank to technical staff of the Centro Integral de Microscopía Electrónica (CIME-CONICET) for their assistance with SEM and SEM-EDS studies. We also thank the technicians Roque Carranza and Juan Oliver for their help in the field work. All experiments, including all animal handling protocols, were carried out in accordance with the Principles of Laboratory Animal Care (National Institutes of Health, publication N° 85-23, revised 1985), as well as specific national laws. All experiments have been examined and approved by the Ethics Committee of Consejo de Investigaciones de Universidad Nacional de Tucumán (CIUNT).

LITERATURE CITED

- Al-Bahry, S.N., I.Y. Mahmoud, K. Melghit, and I. Al-Amri. 2011. Analysis of elemental composition of the eggshell before and after incubation in the Loggerhead Turtle (*Caretta caretta*) in Oman. *Microscopy and Microanalysis* 17:452–460.
- Andrews, R.M., and O.J. Sexton. 1981. Water relations of the eggs of *Anolis auratus* and *Anolis limifrons*. *Ecology* 62:556–562.
- Arias, J.L., D.J. Fink, S.Q. Xiao, A.H. Heuer, and A.I. Caplan. 1993. Biomineralization and eggshells: cell-mediated acellular compartments of mineralized extracellular matrix. *International Review of Cytology* 145:217–250.
- Baer, C.K. 2006. Guidelines on euthanasia of nondomestic animals. American Association of Zoo Veterinarians (AAZV), Yulee, Florida, USA. 111 p.
- Benton, M.J. 2005. *Vertebrate Palaeontology*. 3rd Edition. Blackwell Publishing, Oxford, UK.
- Blackburn, D.G. 1998. Structure, function, and evolution of the oviducts of squamate reptiles, with special reference to viviparity and placentation. *Journal of Experimental Zoology* 282:560–617.
- Blackburn, D.G., and A.F. Flemming. 2009. Morphology, development, and evolution of fetal membranes and placentation in squamate reptiles. *Journal of Experimental Zoology Part B: Molecular and Developmental Evolution* 312:579–589.
- Booth, D.T. 2018. Incubation temperature induced phenotypic plasticity in oviparous reptiles: where to next? *Journal of Experimental Zoology Part A: Ecological and Integrative Physiology* 329:343–350.
- Booth, D., and C. Yu. 2008. Influence of the hydric environment on water exchange and hatchlings of rigid-shelled turtle eggs. *Physiological and Biochemical Zoology* 82:382–387.
- Brizuela, S., and A.M. Albino. 2010. Variaciones dentarias en *Tupinambis merianae* (Squamata: Teiidae). *Cuadernos de Herpetología* 24:5–16.
- Chang, Y., and P.Y. Chen. 2016. Hierarchical structure and mechanical properties of snake (*Naja atra*) and turtle (*Ocadia sinensis*) eggshells. *Acta Biomaterialia* 31:33–49.
- Chardonnet, P., B. Des Clers, J. Fisher, R. Gerhold, F. Jori, and F. Lamarque. 2002. The value of wildlife. *Revue Scientifique et Technique-Office International des Épizooties* 21:15–52.
- Choi, S., S. Han, N-H. Kim, and Y-N. Lee. 2018. A comparative study of eggshells of Gekkota with morphological, chemical compositional and crystallographic approaches and its evolutionary implications. *PLoS ONE* 13:1–31. <https://doi.org/10.1371/journal.pone.0199496>.
- Combes, C., and C. Rey. 2010. Amorphous calcium phosphates: synthesis, properties and uses in biomaterials. *Acta Biomaterialia* 6:3362–3378.
- De La Pierre, M., C. Carteret, L. Maschio, E. André, R. Orlando, and R. Dovesi. 2014. The Raman spectrum of CaCO₃ polymorphs calcite and aragonite: a combined experimental and computational study. *Journal of Chemical Physics* 140:1–12.
- Deeming, D. 1988. The eggshell structure of lizards of two sub-families of the Gekkonidae. *Herpetological Journal* 1:230–234.
- Farmer, C.G. 2003. Reproduction: the adaptive significance of endothermy. *American Naturalist* 162:826–840.
- Fitzgerald, L.A. 2012. Studying and monitoring

- exploited species. Pp. 323–333 *In* Reptile Biodiversity: Standard Methods for Inventory and Monitoring. McDiarmid R.W., M.S. Foster, C. Guyer, N. Chernoff, and J.W. Gibbons (Eds.). University of California Press, Berkeley, California, USA.
- Guillette, L.J., Jr., S.L. Fox, and B.D. Palmer. 1989. Eggshell structure of lizards oviductal morphology and egg shelling in the oviparous lizards *Crotaphytus collaris* and *Eumeces obsoletus*. *Journal of Morphology* 201:145–159.
- Hallmann, K., and E.M. Griebeler. 2015. Eggshell types and their evolutionary correlation with life-history strategies in Squamates. *PLoS ONE* 10:1–20. <https://doi.org/10.1371/journal.pone.0138785>.
- Harvey, M.B., G.N. Ugueto, and R.L. Gutberlet. 2012. Review of Teiid morphology with a revised taxonomy and phylogeny of the Teiidae (Lepidosauria: Squamata). *Zootaxa* 3459:1–156.
- Heulin, B. 1990. Étude comparative de la membrane coquillere chez les souches ovipare et vivipare du lézard *Lacerta vivipara*. *Canadian Journal of Zoology* 68:1015–1019.
- Hirsch, K.F. 1983. Contemporary and fossil chelonian eggshells. *Copeia* 1983:382–397.
- Jarnevich, C.S., M.A. Hayes, L.A. Fitzgerald, A.A. Yackel Adams, B.G. Falk, M.A.M. Collier, L.R. Bonewell, P.E. Klug, S. Naretto, and R.N. Reed. 2018. Modeling the distributions of tegu lizards in native and potential invasive ranges. *Scientific Reports* 8:1–12. <https://doi.org/10.1038/s41598-018-28468-w>.
- Jee, J., B.K. Mohapatra, S.K. Dutta, and G. Sahoo. 2016. Sources of calcium for the agamid lizard *Psammodromus blanfordianus* during embryonic development. *Acta Herpetologica* 11:171–178.
- Karnovsky, M.J. 1965. A formaldehyde-glutaraldehyde fixative of high osmolality for use in electron microscopy. *Journal of Cell Biology* 27:137A.
- Kratochvil, L., and D. Frynta. 2005. Egg shape and size allometry in geckos (Squamata: Gekkota), lizards with contrasting eggshell structure: why lay spherical eggs? *Journal of Zoological Systematics and Evolutionary Research* 44:217–222.
- Kusuda, S., Y. Yasukawa, H. Shibata, T. Saito, O. Doi, Y. Ohya, and N. Yoshizaki. 2013. Diversity in the matrix structure of eggshells in the Testudines (Reptilia). *Zoological Science* 30:366–375.
- Liu, Z., F. Zhang, L. Li, G. Li, W. He, and R.J. Linhardt. 2014. Compositional analysis and structural elucidation of glycosaminoglycans in chicken eggs. *Glycoconjugate Journal* 31:593–602.
- Manes, M.E. 2016. Principles for the Productive Breeding of Tegu Lizards. Bilingual Spanish-English Edition. Facultad de Agronomía y Zootecnia, Universidad Nacional de Tucumán, Tucumán, Argentina.
- Manes, M.E., M.A. Ibañez, and A. Manlla. 2003. Factores físicos y conductas de nidificación de lagartos *Tupinambis merianae* en cautiverio. *Revista Argentina de Producción Animal* 23:119–126.
- Martoja, R., and P.M. Martoja. 1970. Técnicas de Histología Animal. 1ra Edición. Toray-Masson, Barcelona, España.
- Mikhailov, K.E. 1997. Fossil and recent eggshell in amniotic vertebrates: fine structure, comparative morphology and classification. *Special Papers in Palaeontology* 56:1–80.
- Murphy, J.C., M.J. Jowers, R.M. Lehtinen, S.P. Charles, G.R. Colli, A.K. Peres, Jr., C.R. Hendry, and R.A. Pyron. 2016. Cryptic, sympatric diversity in tegu lizards of the *Tupinambis teguixin* group (Squamata, Sauria, Teiidae) and the description of three new species. *PLoS ONE* 11:1–30. <https://doi.org/10.1371/journal.pone.0158542>.
- Muth, A. 1980. Physiological ecology of desert iguana *Dipsosaurus dorsalis* eggs: temperature and water relations. *Ecology* 61:1335–1343.
- Noiva, R.M., A.C. Menezes, and M.C. Peleteiro. 2014. Influence of temperature and humidity manipulation on chicken embryonic development. *BMC Veterinary Research* 10:234. doi: 10.1186/s12917-014-0234-3.
- Norell, M.A., and X. Xu. 2005. Feathered dinosaurs. *Annual Review of Earth and Planetary Sciences* 33:277–299.
- Norman, D.R. 1987. Man and tegu lizards in eastern Paraguay. *Biological Conservation* 41: 39–56.
- Nosenko, V.V., A.M. Yaremko, V.M. Dzhagan, I.P. Vorona, Y.A. Romanyuk, and I.V. Zatovsky. 2016. Nature of some features in Raman spectra of hydroxyapatite-containing materials. *Journal of Raman Spectroscopy* 47:726–730.
- Osborne, L., and M.B. Thompson. 2005. Chemical composition and structure of the eggshell of three viviparous lizards. *Copeia* 2005:683–692.
- Ospina, E.A., L. Merrill and T.J. Benson. 2018. Incubation temperature impacts nestling growth and survival in an open-cup nesting passerine. *Ecology and Evolution* 8:3270–3279.
- Packard, G.C. 1991. Physiological and ecological importance of water to embryos of oviparous reptiles. Pp. 213–228 *In* Egg Incubation: Its Effects on Embryonic Development in Birds and Reptiles. Deeming, D.C., and M.W.J. Ferguson (Eds.). Cambridge University Press, Cambridge, UK.
- Packard, G.C., and M.J. Packard. 1980. Evolution of the cleidoic egg among reptilian antecedents of birds. *American Zoologist* 20:351–362.
- Packard, G.C., M.J. Packard, T.J. Boardman, and M.D. Ashem. 1981. Possible adaptive value of water exchanges in flexible-shelled eggs of turtles. *Science*

- 213:471–473.
- Packard, M.J. 1980. Ultrastructural morphology of the shell and shell membrane of eggs of common snapping turtles (*Chelydra serpentina*). *Journal of Morphology* 165:187–204.
- Packard, M.J., and N.B. Clark. 1996. Aspects of calcium regulation in embryonic Lepidosaurians and chelonians and a review of calcium regulation in embryonic Archosaurians. *Physiological Zoology* 69:435–466.
- Packard, M.J., and V. DeMarco. 1991. Eggshell structure and formation in eggs of oviparous reptiles. Pp. 53–69 *In* Egg Incubation: Its Effects on Embryonic Development in Birds and Reptiles. Deeming, D.C., and M.W.J. Ferguson (Eds.). Cambridge University Press, Cambridge, UK.
- Packard, M.J., and K.F. Hirsch. 1989. Structure of shells from eggs of the geckos *Gekko gekko* and *Phelsuma madagascarensis*. *Canadian Journal of Zoology* 67:746–758.
- Packard, M.J., L.K. Burns, K.F. Hirsch, and G.C. Packard. 1982a. Structure of shells of eggs of *Callisaurus draconoides* (Reptilia, Squamata, Iguanidae). *Zoological Journal of the Linnean Society* 75:297–316.
- Packard, M.J., G.C. Packard, and T.J. Boardman. 1982b. Structure of eggshells and water relations of reptilian eggs. *Herpetologica* 38:136–155.
- Pike, D.A., R.M. Andrews, and W.G. Du. 2012. Eggshell morphology and gekkotan life-history evolution. *Evolutionary Ecology* 26:847–861.
- Pyron, R.A., F.T. Burbrink, and J.J. Wiens. 2013. A phylogeny and revised classification of Squamata, including 4161 species of lizards and snakes. *BMC Evolutionary Biology* 13:1-53. <https://doi.org/10.1186/1471-2148-13-93>.
- Reisz, R.R. 1997. The origin and early evolutionary history of amniotes. *Trends in Ecology & Evolution* 12:218–222.
- Rodríguez-Navarro, A.B., N. Domínguez-Gasca, A. Muñoz, and M. Ortega-Huertas. 2013. Change in the chicken eggshell cuticle with hen age and egg freshness. *Poultry Science* 92:3026–3035.
- Rogers, M.A., L. Langbein, S. Praetzel-Wunder, H. Winter, and J. Schweizer. 2006. Human hair keratin-associated proteins (KAPs). *International Review of Cytology* 251:209–263.
- Roussel, P., G. Lamblin, M. Lhermitte, N. Houdret, J.J. Lafitte, J.M. Perini, A. Klein, and A. Scharfman. 1988. The complexity of mucins. *Biochimie* 70:1471–1482.
- Saber-Samandari, S., K. Alamara, and S. Saber-Samandari. 2014. Calcium phosphate coatings: morphology, micro-structure and mechanical properties. *Ceramics International* 40:563–572.
- Sahoo, G., B.K. Mohapatra, and S.K. Dutta. 2009. Structural changes in Olive Ridley Turtle eggshells during embryonic development. *Herpetological Journal* 19:143–149.
- Schleich, H.H., and W. Kästle. 1988. Reptile Egg-shells SEM Atlas. Gustav Fischer, Stuttgart, Germany.
- Sexton, O.J., J.E. Bramble, I.L. Heisler, C.A. Phillips, and D.L. Cox. 2005. Eggshell composition of squamate reptiles: relationship between eggshell permeability and amino acid distribution. *Journal of Chemical Ecology* 31:2391–2401.
- Sexton, O.J., G.M. Veith, and D.M. Phillips. 1979. Ultrastructure of the eggshell of two species of anoline lizards. *Journal of Experimental Zoology* 207:227–236.
- Silyn-Roberts, H., and R.M. Sharp. 1985. Preferred orientation of calcite and aragonite in the reptilian eggshells. *Proceedings of the Royal Society of London, Series B, Biological Sciences* 225:445–455.
- Silyn-Roberts, H., and R.M. Sharp. 1986. Crystal growth and the role of the organic network in eggshell biomineralization. *Proceedings of the Royal Society of London, Series B, Biological Sciences* 227:303–324.
- Stammeier, J.A., B. Purgstaller, D. Hippler, V. Mavromatis, and M. Dietzel. 2018. *In-situ* Raman spectroscopy of amorphous calcium phosphate to crystalline hydroxyapatite transformation. *MethodsX* 5:1241–1250.
- Stein, K., E. Prondvai, T. Huang, J.M. Baele, P.M. Sander, and R. Reisz. 2019. Structure and evolutionary implications of the earliest (Sinemurian, Early Jurassic) dinosaur eggs and eggshells. *Scientific Reports* 9:1-9. <https://doi.org/10.1038/s41598-019-40604-8>.
- Stewart, J.R. 1997. Morphology and evolution of the egg of oviparous amniotes. Pp. 291–326 *In* Amniote Origins. Sumida, S.S., and K.L.M. Martin (Eds.). Academic Press, San Diego, California, USA.
- Stewart, J.R., and T.W. Ecyay. 2010. Patterns of maternal provision and embryonic mobilization of calcium in oviparous and viviparous squamate reptiles. *Herpetological Conservation and Biology* 5:341–359.
- Stewart, J.R., T.W. Ecyay, and D.G. Blackburn. 2004. Sources and timing of calcium mobilization during embryonic development of the Corn Snake, *Pantherophis guttatus*. *Comparative Biochemistry and Physiology Part A: Molecular & Integrative Physiology* 139:335–341.
- Stewart, J.R., R.A. Pyles, K.A. Mathis, and T.W. Ecyay. 2019. Facultative mobilization of eggshell calcium promotes embryonic growth in an oviparous snake. *Journal of Experimental Biology* 222:jeb193565. <https://doi.org/10.1242/jeb.193565>

- Suvarna, K., C. Layton, and J.D. Bancroft. 2008. Bancroft's Theory and Practice of Histological Techniques. 7th Edition. Churchill Livingstone Elsevier, London, UK.
- Tang, W., B. Zhao, Y. Chen, and W. Du. 2018. Reduced egg shell permeability affects embryonic development and hatchling traits in *Lycodon rufozonatum* and *Pelodiscus sinensis*. *Integrative Zoology* 13:58–69.
- Tattersall, G.J., C.A. Leite, C.E. Sanders, V. Cadena, D.V. Andrade, A.S. Abe, and W.K. Milsom. 2016. Seasonal reproductive endothermy in tegu lizards. *Science Advances* 2:1-7. <https://doi.org/10.1126/sciadv.1500951>.
- Timchenko, P.E., E.V. Timchenko, E.V. Pisareva, M. Y. Vlasov, L.T. Volova, O.O. Frolov, and A.R. Kalimullina. 2018. Experimental studies of hydroxyapatite by Raman spectroscopy. *Journal of Optical Technology* 85:130–135.
- Trauth, S.E., and W.R. Fagerberg. 1984. Ultrastructure and stereology of the eggshell in *Cnemidophorus sexlineatus* (Lacertilia: Teiidae). *Copeia* 1984:826–832.
- Trauth, S.E., C.T. McAllister, and W. Chen. 1994. Microscopic eggshell characteristics in the Collared Lizard, *Crotaphytus collaris* (Sauria: Crotaphytidae). *Southwestern Naturalist* 39:45–52.
- Vieites, C.M., O.M. González, and C.A. Seery. 2007. Análisis de Producciones Animales Alternativas con Potencial de Desarrollo Inmediato y Mediato en la República Argentina. Secretaría de Agricultura, Ganadería y Pesca, Buenos Aires, Argentina. Facultad de Agronomía, Universidad de Buenos Aires. Editorial Gráfica Tres Tiempos, Buenos Aires. Brasil.
- Vinegar, A. 1974. Evolutionary implications of temperature induced anomalies of development in snake embryos. *Herpetologica* 30:72–74.
- Wedral, E.M., D.V. Vadehra, and R.C. Baker. 1974. Chemical composition of the cuticle, and the inner and outer shell membranes from eggs of *Gallus gallus*. *Comparative Biochemistry and Physiology Part B: Comparative Biochemistry* 47:631–640.
- Yoshizaki, N., O. Doi, and N. Uto. 2004. Structure of shell membranes and water permeability in eggs of the Chinese Soft-shelled Turtle *Pelodiscus sinensis* (Reptilia: Trionychidae). *Current Herpetology* 23:1–6.
- Zhang, J., L. Tang, H. Qi, Q. Zhao, Y. Liu, and Y. Zhang. 2019. Dual function of magnesium in bone biomineralization. *Advanced Healthcare Materials* 8(21):1-12. <http://doi: 10.1002/adhm.201901030>.
- Zhao, B., Y. Chen, Y. Wang, P. Ding, and W.G. Du. 2013. Does the hydric environment affect the incubation of small rigid-shelled turtle eggs? *Comparative Biochemistry and Physiology Part A: Molecular & Integrative Physiology* 164:66–70.



FERNANDO CAMPOS-CASAL completed his undergraduate course in Biological Sciences and received a Ph.D. degree in Biological Sciences (Zoology), both from the Facultad de Ciencias Naturales e Instituto Miguel Lillo de la Universidad Nacional de Tucumán, Tucumán, Argentina. He is currently a Professor of Developmental Biology at Facultad de Agronomía y Zootecnia de la Universidad Nacional de Tucumán. He has experience in the field of Zoology, with emphasis on early development of amphibians and reptiles, morphology and histology. (Photographed by Eliana Gomez).



FRANCISCO CORTEZ is a Zootechnics Engineer and is currently a Professor at Facultad de Agronomía y Zootecnia de la Universidad Nacional de Tucumán, Argentina. He has experience in techniques to determine sex early in development, and the breeding and management of tegu lizards in captivity. (Photographed by Eliana Gomez).



ELIANA GOMEZ is a Zootechnics Engineer and is currently a Professor at Facultad de Agronomía y Zootecnia de la Universidad Nacional de Tucumán, Argentina. She has experience in breeding and management of tegu lizards in captivity. (Photographed by Fernando Campos-Casal).



SILVIA CHAMUT has a Ph.D. degree in Biological Sciences and is an Associate Professor in the Department of Development Biology of the Facultad de Agronomía y Zootecnia, Universidad Nacional de Tucumán, Argentina. Her research is focused on the reproductive biology and metabolism of *Salvator* lizards bred in captivity. (Photographed by Fernando Campos-Casal).